Progress In Electromagnetics Research, *PIER 31, 181–193, 2001*

NEAR FIELDS OF ELECTRICALLY SMALL THIN SQUARE AND RECTANGULAR LOOP ANTENNAS

L.-W. Li, C.-P. Lim, and M.-S. Leong

Communication and Microwave Division
Department of Electrical and Computer Engineering
National University of Singapore
10 Kent Ridge Crescent, Singapore 119260

Abstract–This paper presents an alternative vector analysis of the electromagnetic (EM) fields radiated from electrically small thin square and rectangular loop antennas of arbitrary length $2a$ and width $2b$. This method employs the dyadic Green's function (DGF) in the derivation of the EM radiated fields and thus makes the analysis general, compact and straightforward. Both near- and far-zones are considered so that the EM radiated fields are expressed in terms of the vector wave eigenfunctions. Not only the exact solution of the EM fields in the near and far zones outside the region (where $r > \sqrt{a^2 + b^2}$) is derived by use of spherical Hankel functions of the first kind, but also the closed series form of the EM fields radiated in the near zone inside the region $0 \leq r < b$ is obtained in series of spherical Bessel functions of the first kind. The two regions between the radial distances b and $\sqrt{a^2 + b^2}$ which are defined as intermediate zones are characterized by both the spherical Bessel and Hankel functions of the first kind. Validity of the numerical results is discussed and clarified.

1. INTRODUCTION

Thin circular loop antennas carrying different forms of the currents and their radiation characteristics have been extensively investigated and well-documented by many researchers in over the last several decades, e.g., [1–20], to the authors' knowledge. The radiation characteristics of circular loop antennas can be readily found from antenna text books [21, 22]. However, literature on polygonal loop antennas located in free-space is limited [23–28]. It was cited in [25] that "theoretical analysis seems to be unsuccessful" for rectangular loops and therefore further analysis of the rectangular loop antennas has received less attention. In [24], the rectangular loop antennas were modeled as a dipole and the work was extremely complicated and radiation patterns were not given. In [23], only experimental techniques and measurements were presented. Recently, Jensen et al. presented their work [26] on rectangular loops as an extreme case in their analysis, where superquadric geometries were used to model the rectangular perimeter. In [21], only approximated current distribution is used to show the radiation patterns in far zone whereas in [22], a constant current was treated in the problem. For the near-zone fields, none has been reported in the literature, to the authors' knowledge. This is partially due to the difficulty in evaluating integrals analytically. Therefore, this paper aims to present exact solutions of the electromagnetic fields in both near, far and intermediate zones using the DGF technique for the square and rectangular loop antennas.

2. GENERAL FORMULATION OF EM RADIATED FIELDS

Fig. 1 shows the geometry of a thin rectangular loop antenna located at $z = 0$. The current distribution along the loop, i.e, I_0, is assumed to be constant for electrically small loop antennas.

The detailed formulation of the EM radiated fields of circular loop antennas has been shown in [19, Eqs. (1)–(7)]. In view of this, the authors will not repeat the procedure. The inner, outer and intermediate regions defined in this paper are depicted in Fig. 2. Given the constant current distribution, we can obtain the EM field expressions for the four zones after substituting spherical dyadic Green's functions

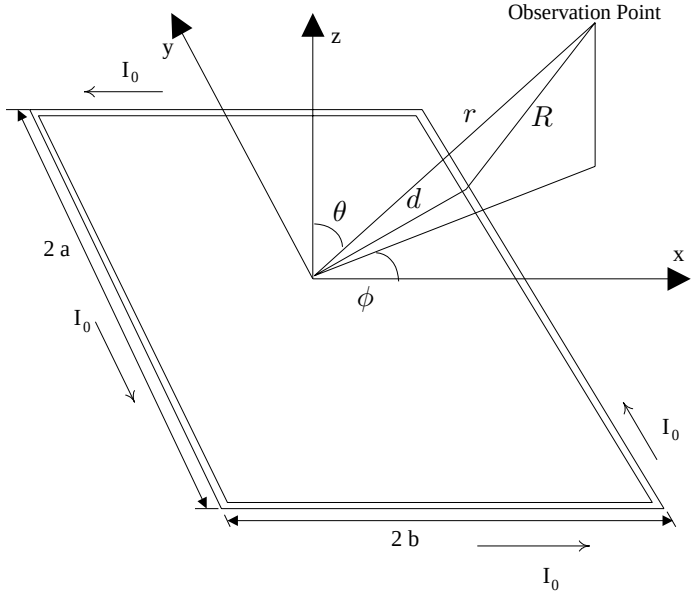

Figure 1. Geometry of a thin rectangular loop antenna.

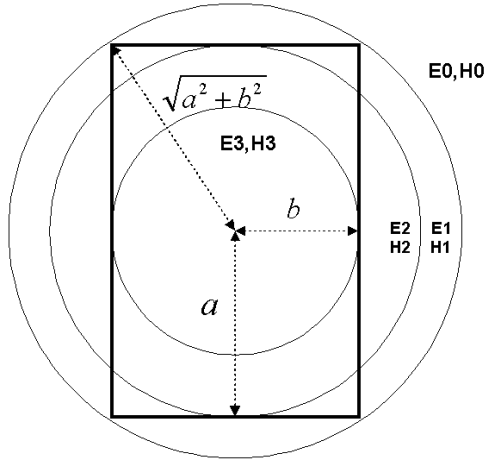

Figure 2. Intermediated zones.

into the field representation as follows:

$$\begin{bmatrix} E_{0,r} \\ E_{1,r} \\ E_{2,r} \\ E_{3,r} \end{bmatrix} = -\frac{\eta_0 k_0^2}{4\pi} \sum_{n=1}^{\infty} D_n P_n(\cos\theta) \frac{n(n+1)}{k_0 r} \cdot \left\{ j_n(k_0 r) \begin{bmatrix} 0 \\ (\Phi_n^{N,1>}) \\ (\Phi_n^{N,2>}) \\ (\Phi_n^{N,3>}) \end{bmatrix} + h_n^{(1)}(k_0 r) \begin{bmatrix} (\Phi_n^{N,0<}) \\ (\Phi_n^{N,1<}) \\ (\Phi_n^{N,2<}) \\ 0 \end{bmatrix} \right\}, \quad (1a)$$

$$\begin{bmatrix} E_{0,\theta} \\ E_{1,\theta} \\ E_{2,\theta} \\ E_{3,\theta} \end{bmatrix} = -\frac{\eta_0 k_0^2}{4\pi} \sum_{n=1}^{\infty} D_n \frac{dP_n(\cos\theta)}{d\theta} \left\{ \frac{d[r j_n(k_0 r)]}{k_0 r dr} \begin{bmatrix} 0 \\ (\Phi_n^{N,1>}) \\ (\Phi_n^{N,2>}) \\ (\Phi_n^{N,3>}) \end{bmatrix} + \frac{d[r h_n^{(1)}(k_0 r)]}{k_0 r dr} \begin{bmatrix} (\Phi_n^{N,0<}) \\ (\Phi_n^{N,1<}) \\ (\Phi_n^{N,2<}) \\ 0 \end{bmatrix} \right\}, \quad (1b)$$

$$\begin{bmatrix} E_{0,\phi} \\ E_{1,\phi} \\ E_{2,\phi} \\ E_{3,\phi} \end{bmatrix} = -\frac{\eta_0 k_0^2}{4\pi} \sum_{n=1}^{\infty} -D_n \frac{dP_n(\cos\theta)}{d\theta} \cdot \left\{ j_n(k_0 r) \begin{bmatrix} 0 \\ \Phi_n^{M,1>} \\ \Phi_n^{M,2>} \\ \Phi_n^{M,3>} \end{bmatrix} + h_n^{(1)}(k_0 r) \begin{bmatrix} \Phi_n^{M,0<} \\ \Phi_n^{M,1<} \\ \Phi_n^{M,2<} \\ 0 \end{bmatrix} \right\}, \quad (1c)$$

where $j_n(k_0 r)$ and $h_n^{(1)}(k_0 r)$ are the spherical Bessel and Hankel functions of the first kind, respectively, $P_n(\cos\theta)$ is the Legendre function, and the normalization coefficient D_n of Legendre polynomials is defined by

$$D_n = \frac{(2n+1)}{n(n+1)}. \quad (2)$$

The coefficients of the EM fields are expressed by

$$\Phi_n^* = \Psi_{e13}^* + \Psi_{e24}^*, \quad (3)$$

which are listed in Appendix.

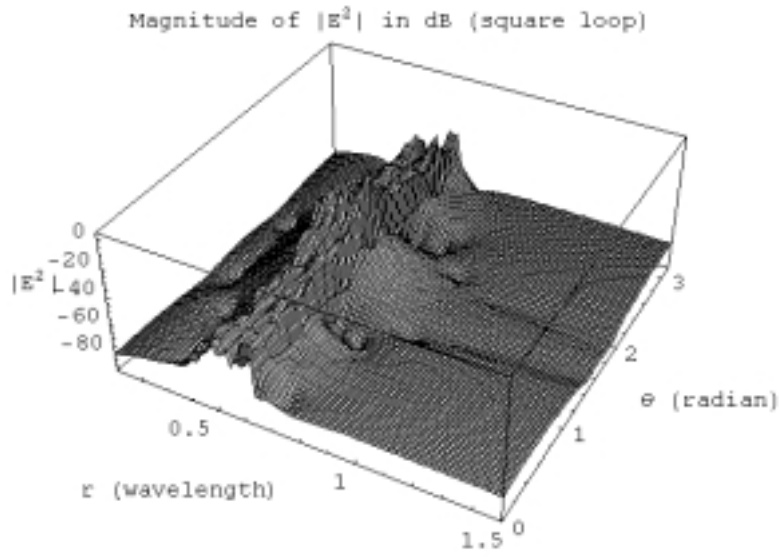

Figure 3. Power intensity (in dB) of the square loop $(0.5\lambda$ by $0.5\lambda)$ antenna as a function of r and θ in E and H planes.

3. NUMERICAL RESULTS

For square loop antennas, intermediate length $2a$ and width $2b$ are equal and therefore, only one intermediate region exists. As a result, $\boldsymbol{E}_2$ and $\boldsymbol{H}_2$ disappear whereas $\boldsymbol{E}_1$ and $\boldsymbol{H}_1$ are applicable in characterizing the fields in the intermediate region. The EM fields in inner, outer and intermediate regions for square and rectangular loop antennas are obtained using the DGF. Four hundred terms are considered for the numerical computation of the summation of the spherical Bessel and Hankel functions (i.e., with respect to the index n) for which convergence has been satisfactorily achieved. The power intensities in 3-D plots over the regions of the rectangular and square loop antennas are depicted in Figs. 3 to 8, respectively. The figures clearly show that the magnitudes of field intensities increase as the observation point moves closer to the source and decreases as it moves away. Besides, it is obvious that the directivity increases too, as the observation point gets closer to the source. All these observations, by instinct and intuition, are correct. At the coordinate origin (center of the square loop), the electromagnetic fields become null, which is in agreement with the result of the Bourt theorem for magneto-static cases. Due to the sym-

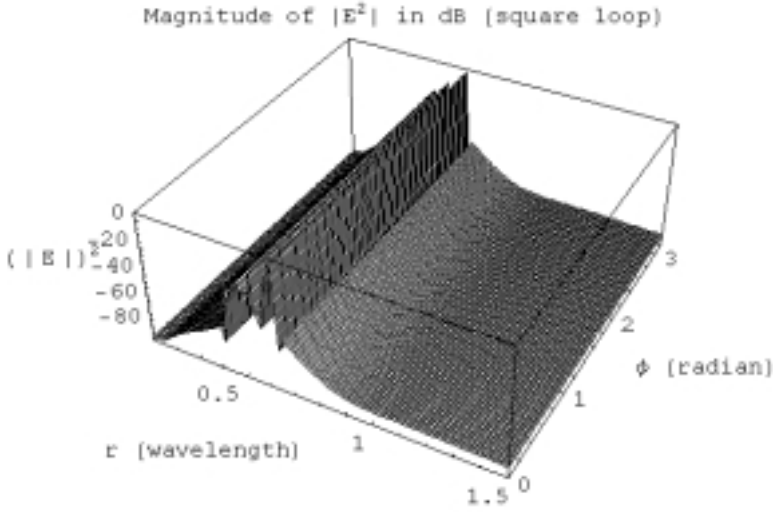

Figure 4. Power intensity (in dB) of the square loop (0.5λ by 0.5λ) antenna as a function of r and ϕ in $X\,Y$ plane.

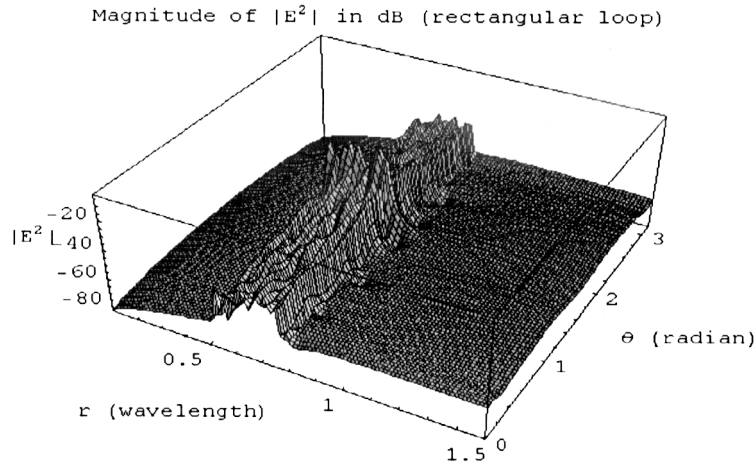

Figure 5. Power intensity (in dB) of the rectangular loop (0.6λ by 0.5λ) antenna as a function of r and θ in E- and H-planes.

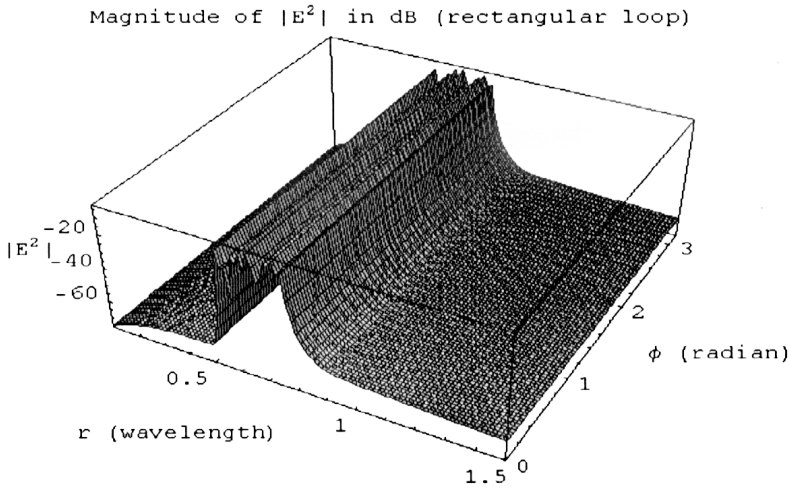

Figure 6. Power intensity (in dB) of the rectangular loop (0.6λ by 0.5λ) antenna as a function of r and ϕ in X-Y plane.

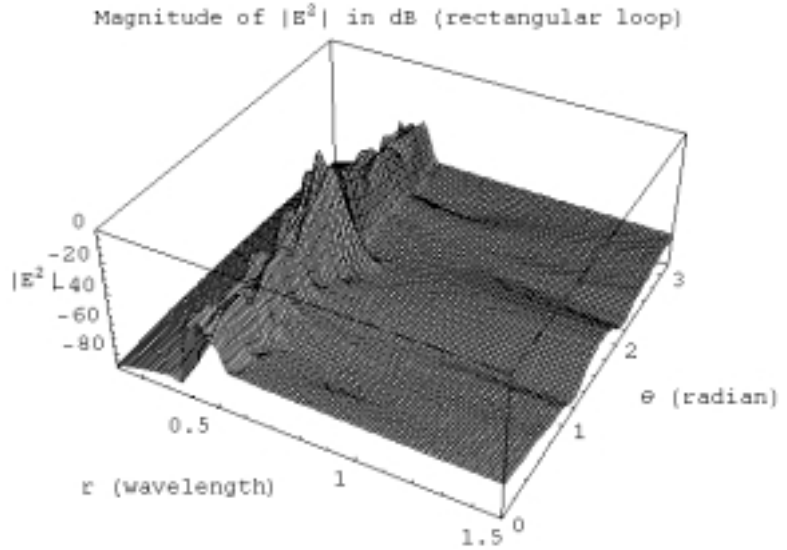

Figure 7. Power intensity (in dB) of the rectangular loop (0.5λ by 0.25λ) antenna as a function of r and θ in E- and H-planes.

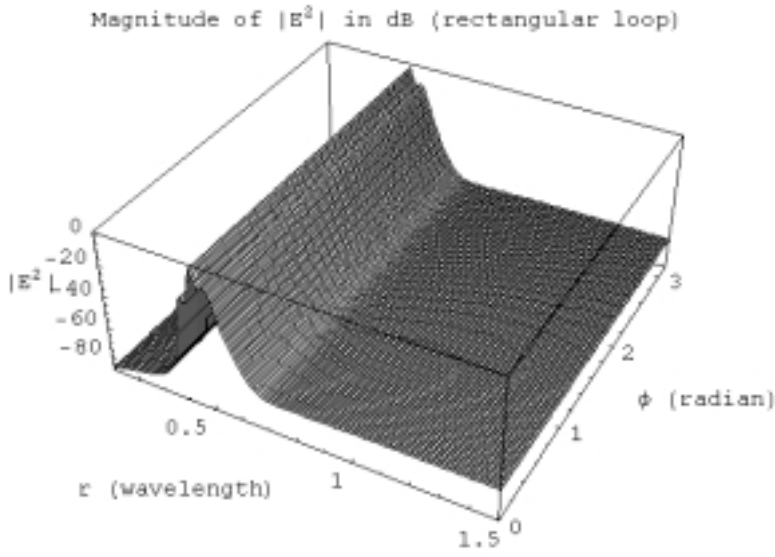

Figure 8. Power intensity (in dB) of the rectangular loop (0.5λ by 0.25λ) antenna as a function of r and ϕ in X-Y plane.

metry of E- and H-planes, only one of them is considered here. From Figs. 3 to 8, it is also seen that around the loop, the electric fields reach a maximum, and the field distribution due to the loop varies dramatically with the location, especially within the area of regions 2 and 3. This phenomenon is primarily due to multiple interactions of the source current and the radiated field; and strong couplings within the reactive region are observed. Besides this, we can observe from Figs. 3 and 5 or Figs. 4 and 6 that continuities exist though both are characterized quite differently. This, in some sense, shows that the derivation is correct. The numerical results for radiation patterns in the far-field are also compared with results obtained in [21, Fig. 5.52] and an excellent agreement between the two results is obtained. This confirms partially the correctness of our theoretical derivation and numerical algorithm.

4. CONCLUSIONS

This paper characterizes the radiated electromagnetic fields within the inner, outer and intermediate regions in the near-zone due to thin

square and rectangular loop antennas. To obtain the exact expressions of the electromagnetic fields in the near, far and intermediate regions, the dyadic Green's function in spherical coordinates is utilized and the radiation patterns due to rectangular/square loops carrying a uniform current distribution are plotted. Some new results of antenna patterns are also presented in the paper in the near zones and necessary discussions are made.

APPENDIX. EXPLICIT EXPRESSIONS OF COEFFICIENTS OF THE SERIES

The intermediate expressions of the coefficients defined in (1a)–(1c) are determined as follows:

$$\begin{bmatrix} \Psi_{e13}^{M,0<} \\ \Psi_{e13}^{M,1<} \\ \Psi_{e13}^{M,1>} \\ \Psi_{e13}^{M,2<} \\ \Psi_{e13}^{M,2>} \\ \Psi_{e13}^{M,3>} \end{bmatrix}$$

$$= \begin{bmatrix} (\int_{-\phi_0}^{\phi_0} + \int_{\pi-\phi_0}^{\pi+\phi_0}) j_n(\frac{k_0 a}{|\cos\phi'|}) \\ (\int_{-\frac{\pi}{2}+\phi_1}^{\frac{\pi}{2}-\phi_1} + \int_{\frac{\pi}{2}+\phi_1}^{\frac{3\pi}{2}-\phi_1}) j_n(\frac{k_0 a}{|\cos\phi'|}) \\ (\int_{2\pi-\phi_0}^{-\frac{\pi}{2}+\phi_1} + \int_{\frac{\pi}{2}-\phi_1}^{\phi_0}) h_n^{(1)}(\frac{k_0 a}{|\cos\phi'|}) + (\int_{\pi-\phi_0}^{\frac{\pi}{2}+\phi_1} + \int_{\frac{3\pi}{2}-\phi_1}^{\pi+\phi_0}) h_n^{(1)}(\frac{k_0 a}{|\cos\phi'|}) \\ (\int_{-\frac{\pi}{2}+\phi_1}^{\frac{\pi}{2}-\phi_1} + \int_{\frac{\pi}{2}+\phi_1}^{\frac{3\pi}{2}-\phi_1}) j_n(\frac{k_0 a}{|\cos\phi'|}) \\ (\int_{2\pi-\phi_0}^{-\frac{\pi}{2}+\phi_1} + \int_{\frac{\pi}{2}-\phi_1}^{\phi_0}) h_n^{(1)}(\frac{k_0 a}{|\cos\phi'|}) + (\int_{\pi-\phi_0}^{\frac{\pi}{2}+\phi_1} + \int_{\frac{3\pi}{2}-\phi_1}^{\pi+\phi_0}) h_n^{(1)}(\frac{k_0 a}{|\cos\phi'|}) \\ (\int_{-\phi_0}^{\phi_0} + \int_{\pi-\phi_0}^{\pi+\phi_0}) h_n^{(1)}(\frac{k_0 a}{|\cos\phi'|}) \end{bmatrix}$$

$$\cdot \left\{ -I_0 \cos(\phi') \frac{dP_n(0)}{d\theta} \left(\frac{a}{|\cos\phi'|} \right)^2 \right\} d\phi', \tag{4a}$$

$$\begin{bmatrix} \Psi_{e24}^{M,0<} \\ \Psi_{e24}^{M,1<} \\ \Psi_{e24}^{M,1>} \\ \Psi_{e24}^{M,2<} \\ \Psi_{e24}^{M,2>} \\ \Psi_{e24}^{M,3>} \end{bmatrix}$$

$$= \begin{bmatrix} (\int_{\phi_0}^{\pi-\phi_0} + \int_{\pi+\phi_0}^{2\pi-\phi_0}) j_n(\frac{k_0 b}{|\sin\phi'|}) \\ (\int_{\frac{\pi}{2}-\phi_2}^{\frac{\pi}{2}+\phi_2} + \int_{\frac{3\pi}{2}-\phi_2}^{\frac{3\pi}{2}+\phi_2}) j_n(\frac{k_0 b}{|\sin\phi'|}) \\ (\int_{\phi_0}^{\frac{\pi}{2}-\phi_2} + \int_{\frac{\pi}{2}+\phi_2}^{\pi-\phi_0}) h_n^{(1)}(\frac{k_0 b}{|\sin\phi'|}) + (\int_{\frac{3\pi}{2}+\phi_2}^{2\pi-\phi_0} + \int_{\pi+\phi_0}^{\frac{3\pi}{2}-\phi_2}) h_n^{(1)}(\frac{k_0 b}{|\sin\phi'|}) \\ 0 \\ (\int_{\phi_0}^{\pi-\phi_0} + \int_{\pi+\phi_0}^{2\pi-\phi_0}) h_n^{(1)}(\frac{k_0 b}{|\sin\phi'|}) \\ (\int_{\phi_0}^{\pi-\phi_0} + \int_{\pi+\phi_0}^{2\pi-\phi_0}) h_n^{(1)}(\frac{k_0 b}{|\sin\phi'|}) \end{bmatrix}$$

$$\cdot \left\{ -I_0 \sin(\phi') \frac{dP_n(0)}{d\theta} \left(\frac{b}{|\sin\phi'|} \right)^2 d\phi' \right\}, \tag{4b}$$

$$\begin{bmatrix} \Psi_{e13}^{N,0<} \\ \Psi_{e13}^{N,1<} \\ \Psi_{e13}^{N,1>} \\ \Psi_{e13}^{N,2<} \\ \Psi_{e13}^{N,2>} \\ \Psi_{e13}^{N,3>} \end{bmatrix}$$

$$= \begin{bmatrix} (\int_{-\phi_0}^{\phi_0} + \int_{\pi-\phi_0}^{\pi+\phi_0}) j_n(\frac{k_0 a}{|\cos\phi'|}) \\ (\int_{-\frac{\pi}{2}+\phi_1}^{\frac{\pi}{2}-\phi_1} + \int_{\frac{\pi}{2}+\phi_1}^{\frac{3\pi}{2}-\phi_1}) j_n(\frac{k_0 a}{|\cos\phi'|}) \\ (\int_{2\pi-\phi_0}^{-\frac{\pi}{2}+\phi_1} + \int_{\frac{\pi}{2}-\phi_1}^{\phi_0}) h_n^{(1)}(\frac{k_0 a}{|\cos\phi'|}) + (\int_{\pi-\phi_0}^{\frac{\pi}{2}+\phi_1} + \int_{\frac{3\pi}{2}-\phi_1}^{\pi+\phi_0}) h_n^{(1)}(\frac{k_0 a}{|\cos\phi'|}) \\ (\int_{-\frac{\pi}{2}+\phi_1}^{\frac{\pi}{2}-\phi_1} + \int_{\frac{\pi}{2}+\phi_1}^{\frac{3\pi}{2}-\phi_1}) j_n(\frac{k_0 a}{|\cos\phi'|}) \\ (\int_{2\pi-\phi_0}^{-\frac{\pi}{2}+\phi_1} + \int_{\frac{\pi}{2}-\phi_1}^{\phi_0}) h_n^{(1)}(\frac{k_0 a}{|\cos\phi'|}) + (\int_{\pi-\phi_0}^{\frac{\pi}{2}+\phi_1} + \int_{\frac{3\pi}{2}-\phi_1}^{\pi+\phi_0}) h_n^{(1)}(\frac{k_0 a}{|\cos\phi'|}) \\ (\int_{-\phi_0}^{\phi_0} + \int_{\pi-\phi_0}^{\pi+\phi_0}) h_n^{(1)}(\frac{k_0 a}{|\cos\phi'|}) \end{bmatrix}$$

$$\cdot \left\{ I_0 \sin(\phi') \frac{n(n+1)P_n(0)}{k_0} \frac{a}{|\cos\phi'|} d\phi' \right\}, \tag{4c}$$

$$\begin{bmatrix} \Psi_{e24}^{N,0<} \\ \Psi_{e24}^{N,1<} \\ \Psi_{e24}^{N,1>} \\ \Psi_{e24}^{N,2<} \\ \Psi_{e24}^{N,2>} \\ \Psi_{e24}^{N,3>} \end{bmatrix}$$

$$= \begin{bmatrix} (\int_{\phi_0}^{\pi-\phi_0} + \int_{\pi+\phi_0}^{2\pi-\phi_0}) j_n(\frac{k_0 b}{|\sin\phi'|}) \\ (\int_{\frac{\pi}{2}-\phi_2}^{\frac{\pi}{2}+\phi_2} + \int_{\frac{3\pi}{2}-\phi_2}^{\frac{3\pi}{2}+\phi_2}) j_n(\frac{k_0 b}{|\sin\phi'|}) \\ (\int_{\phi_0}^{\frac{\pi}{2}-\phi_2} + \int_{\frac{\pi}{2}+\phi_2}^{\pi-\phi_0}) h_n^{(1)}(\frac{k_0 b}{|\sin\phi'|}) + (\int_{\frac{3\pi}{2}+\phi_2}^{2\pi-\phi_0} + \int_{\pi+\phi_0}^{\frac{3\pi}{2}-\phi_2}) h_n^{(1)}(\frac{k_0 b}{|\sin\phi'|}) \\ 0 \\ (\int_{\phi_0}^{\pi-\phi_0} + \int_{\pi+\phi_0}^{2\pi-\phi_0}) h_n^{(1)}(\frac{k_0 b}{|\sin\phi'|}) \\ (\int_{\phi_0}^{\pi-\phi_0} + \int_{\pi+\phi_0}^{2\pi-\phi_0}) h_n^{(1)}(\frac{k_0 b}{|\sin\phi'|}) \end{bmatrix}$$

$$\cdot \left\{ I_0 \cos(\phi') \frac{n(n+1) P_n(0)}{k_0} \frac{b}{|\sin\phi'|} d\phi' \right\}. \tag{4d}$$

REFERENCES

1. Kanda, M., "An electromagnetic near-field sensor for simultaneous electric and magnetic-field measurements," *IEEE Trans. Electromagn. Compat.,* Vol. EMC-26, No. 3, 102–110, Aug. 1984.
2. Smith, G. S., "On the electrically small bare loop antenna in a dissipative medium," *IEEE Trans. Antennas Propagat.*, Vol. AP-11, 533–537, July 1963.
3. Foster, D., "Loop antennas with uniform current," *Proc. IRE*, Vol. 32, 603–607, Oct. 1944.
4. Iizuka, K., "The circular loop antenna multiloaded with positive and negative resistors," *IEEE Trans. Antennas Propagat.,* Vol. AP-13, 7–20, Jan. 1965.
5. Wu, T. T., "Theory of the thin circular antenna," *J. Math. Phys.,* Vol. 3, 1301–1304, Dec. 1962.
6. Mei, K. K., "On the integral equations of thin wire antennas," *IEEE Trans. Antennas Propagat.,* Vol. AP-13, No. 3, 374–378, May 1965.
7. Blackburn, R. F. and D. R. Wilton, "Analysis and synthesis of an impedance-loaded loop antenna using the singularity expansion method," *IEEE Trans. Antennas Propagat.,* Vol. AP-26, No. 1, 136–140, Jan. 1978.

8. Glinski, G., "Note on the circular loop antennas with nonuniform current distribution," *J. Appl. Phys.,* Vol. 18, 638–644, July 1947.
9. Richtscheid, A., "Calculation of the radiation resistance of loop antennas with sinusoidal current distribution," *IEEE Trans. Antennas Propagat.,* 889–891, Nov. 1976.
10. Esselle, K. P. and S. S. Stuchly, "Resistively loaded loop as a pulse-receiving antenna," *IEEE Trans. Antennas Propagat.,* Vol. 38, No. 7, 1123–1126, July 1990.
11. Zhou, G. P. and G. S. Smith, "An accurate theoretical model for thin-wire circular half-loop antenna," *IEEE Trans. Antennas Propagat.,* Vol. 39, No. 8, 1167–1177, Aug. 1991.
12. Tsai, L. L., "A numerical solution for the near and far fields of an annular ring of magnetic current," *IEEE Trans. Antennas Propagat.,* Vol. AP-20, No. 5, 569–576, Sept. 1972.
13. Rao, B. R., "Far Field Patterns of large circular loop antennas: Theoretical and experimental results," *IEEE Trans. Antennas Propagat.,* Vol. AP-16, 269–270, Mar. 1968.
14. Chen, C. L. and R. W. P. King, "The small bare loop antenna immersed in a dissipative medium," *IEEE Trans. Antennas Propagat.,* Vol. AP-11, 266–269, May 1963.
15. Iizuka, K. and F. L. Russa, "Table of the field patterns of a loaded resonant circular loop," *IEEE Trans. Antennas Propagat.,* Vol. AP-18, 416–418, May 1970.
16. Abo-Zena, A. M. and R. E. Beam, "Transient radiation field of a circular loop antenna," *IEEE Trans. Antennas Propagat.,* Vol. AP-20, 380–383, May 1972.
17. Overfelt, P. L., "Near fields of the constant current thin circular loop antenna of arbitrary radius," *IEEE Trans. Antennas Propagat.,* Vol. 44, No. 2, 166–171, Feb. 1996.
18. Werner, D. H., "An exact integration procedure for vector potential of thin circular loop antennas," *IEEE Trans. Antennas Propagat.,* Vol. 44, No. 2, 157–165, Feb. 1996.
19. Li, L. W., M. S. Leong, P. S. Kooi, and T. S. Yeo, "Exact solutions of electromagnetic fields in both near and far zones radiated by thin circular-loop antennas: A general representation," *IEEE Trans. Antennas Propagat.,* Vol. 45, 1741–1748, Dec. 1997.
20. Li, L. W., C. P. Lim, and M. S. Leong, "Method of moments analysis of electrically large circular-loop antennas: Non-uniform currents," *Proc. Inst. Elect. Eng., Pt. H,* Vol. 146, No. 6, 416–420, Dec. 1999.
21. Stutzman, W. L. and G. A. Thiele, *Antenna Theory and Design,* 2nd edition, Wiley, New York, 1998.

22. Balanis, C. A., *Antenna Theory: Analysis and Design,* 2nd edition, Wiley, New York, 1997.
23. Kennedy, P. A., "Loop antenna measurements," *IRE Trans. Antennas Propagat.,* 610–618, Oct. 1956.
24. King, R., "The rectangular loop antennas as a dipole," *IRE Trans. Antennas Propagat.,* 53–61, 1959.
25. Tsukiji, T. and S. Tou, "On polygonal loop antennas," *IEEE Trans. Antennas Propagat.,* Vol. AP-28, No. 4, 571–575, July 1980.
26. Jensen, M. A. and Y. Rahmat-Samii, "Electromagnetic characteristics of superquadric wire loop antennas," *IEEE Trans. Antennas Propagat.,* Vol. 42, No. 2, 264–269, Feb. 1994.
27. Lim, C. P., L. W. Li, and M. S. Leong, "Method of moments analysis of electrically large square and rectangular loop antennas with non-uniform currents," *Proceedings of Antenna Applications Symposium,* 166–182, Monticello, IL, Sep. 1999.
28. Li, L. W., C. P. Lim, and M. S. Leong, "Near-field radiation patterns of electrically small thin rectangular/square loop antennas," *Proceedings of Asia-Pacific Microwave Conference,* 910–913, Singapore, Dec. 1999.